First publ. in: Physica E: Low-dimensional Systems and Nanostructures 21 (2004), 2/4, pp. 646-650

Umklapp process in observation of coherent folded longitudinal acoustic phonons in a GaAs/AlAs long-period superlattice

K. Mizoguchi[1]*, T. Hino[1], M. Nakayama[1], T. Dekorsy[2], A. Bartels[3], H. Kurz[3], and S. Nakashima[4]
[1]Dept. of Applied Physics, Osaka City University, Sumiyoshi-ku, Osaka, 558-8585, Japan.
[2] Forschungszentrum Rossendorf, D-01314 Dresden, 510119,Germany.
[3]Institut für Halbleitertechnik, RWTH Aachen, 52074 Aachen, Germany.
[4]National Institute of Advanced Industrial Science and Technology, Tsukuba 305-8568, Japan.
*Corresponding author: Phone/Fax:+81-6-6605-2174, Email:mizoguch@a-phys.eng.osaka-cu.ac.jp

Abstract: Coherent folded longitudinal acoustic phonons in a GaAs/AlAs long-period superlattice have been investigated by using a reflection-type two-color pump-probe technique under the condition that the wave vector of the probe pulse in the sample exceeds the mini-Brillouin zone. The coherent oscillations observed in the time-domain signals indicate the propagation of the phonon wave packet through the whole superlattice layer. The Fourier transform spectrum of the time-domain signals is compared with the dispersion relation of the folded longitudinal acoustic phonons in the long-period superlattice calculated using a transfer matrix method on the bases of an elastic continuum model. This comparison indicates that the folded longitudinal acoustic phonons in the long-period superlattice are observed through the umklapp process.

Keywords: coherent phonons, umklapp process, GaAs/AlAs superlattice

1. Introduction

A pump-probe technique using an ultrashort pulse laser is a useful technique to study the dynamics of phonons and carriers. The dynamics of coherent folded longitudinal acoustic (FLA) phonons in semiconductor superlattices (SL's) has attracted much attention because the propagating and standing waves of coherent FLA phonons in GaAs/AlAs SLs are directly observed in the time domain [1-4]. The generation and detection mechanisms of coherent phonons have been continuously discussed [5]. Recently, we performed a two-color (2C) pump-probe experiment on GaAs/AlAs SL's, and obtained the result that the wave vector conservation holds only for the probe pulse and coherent phonons in the detection process; namely the wave vector, q, of the propagating FLA phonons is presented by $q=2k_{probe}$, where k_{probe} is the wave vector of probe pulse [3]. Until now, in the investigation for coherent FLA phonons, the wave vector, q, has been limited to the value within the mini-Brillouin zone in a SL. When the value of $2k_{probe}$ exceeds the mini-Brillouin zone, the question may arise as whether we can observe the coherent FLA phonons or not, and what the wave vector of the detected coherent FLA phonons will be.

In this paper, we report on the time-resolved study of coherent FLA phonons in a GaAs/AlAs long-period SL that consists of alternate stacking of a periodic SL layer and AlGaAs layer, using a reflection-type 2C pump-probe technique under the condition that the wave vector of the probe pulse in the long-period SL exceeds the mini-Brillouin zone. The time-domain signals indicate that the coherent oscillations correspond to the propagating phonon wave packet in the long-period SL. The Fourier transform (FT) spectrum of the time-domain signals observed in the long-period SL is compared with the dispersion relation of the FLA phonon calculated using a transfer matrix method based on an elastic continuum model. This comparison demonstrates that the coherent FLA phonons in the long-period SL are observed through an umklapp process.

2. Experimental

A GaAs/AlAs long-period SL was grown on a (001) GaAs substrate by molecular beam epitaxy. As shown in Fig. 1, the structure of the long-period SL consists of alternate stacking of a periodic SL layer and an AlGaAs layer, i.e., a $(GaAs)_{10}(AlAs)_{10}$ SL with 8 periods and an

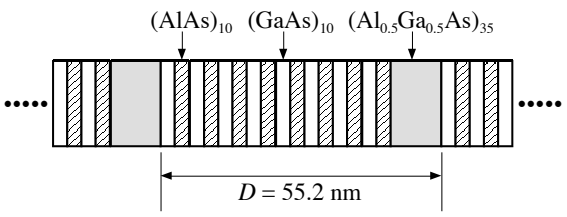

Fig. 1 Schematic diagram of the GaAs/AlAs log-period superlattice.

$(Al_{0.5}Ga_{0.5}As)_{35}$ layer, where the subscripts denote the number of monolayers in constituent layers (one monolayer = 0.283 nm). The thickness of one SL period of this sample is D=55.2 nm, and the total thickness of the whole structure is about 607 nm. In addition, a $(GaAs)_{10}(AlAs)_{10}$ SL with 195 periods, of which the total thickness is about 1104 nm, was used as a reference sample.

The reflection-type 2C pump-probe measurements were performed at room temperature by using a mode-locked Ti:sapphire pulse laser delivering about 100-fs pulses. The probe and pump pulses were the fundamental laser light with the wavelength of 720 nm and its second-harmonic light with the wavelength of 360 nm, respectively. The wavelength of the probe pulse was tuned closely to the first interband transition of the long-period SL, which was determined by a photoreflectance experiment. Under the present experimental condition, the value of $2k_{probe}$ in the sample estimated from the refractive index at 720 nm is larger than that of the zone edge of the mini-Brillouin zone: $q/q_{max} = 2k_{probe}/(\pi/D)$ ~1.07. Here, q_{max} is the zone-edge wave vector π/D, and D is the period of the SL. In this calculation, we assume that the refractive index, n, of the long-period SL is the same as that of $Al_{0.5}Ga_{0.5}As$ (n=3.5 for 720 nm) [6]. The time delay of the probe pulse was adjusted by a variable optical delay line. The time derivative of the reflectivity change, $\partial(\Delta R/R_0)/\partial t$, was recorded by modulating the optical path of the pump pulse with a shaker, in order to highlight the oscillatory component. We extracted only the signals of the FLA phonons by subtracting a slowly varying background due to the sound wave.

3. Results and Discussion

Figure 2 shows the oscillatory components of the time-derivative signals of the reflectivity changes in the long-period SL. The time-domain signal of the $(GaAs)_{10}(AlAs)_{10}$ SL is also depicted in Fig. 1 for reference. In both samples, the time-domain signals show the oscillatory structure exhibiting strong beating. The time periods of the main oscillation and the beat in both the samples are about 1.1 and 10 ps, respectively. The coherent oscillations with a very long dephasing time in the $(GaAs)_{10}(AlAs)_{10}$ SL are observed in the time range more than 140 ps, while those in the long-period SL gradually dephase and suddenly disappear after about 115 ps.

The time-domain signals in both the SL's observed by using the 2C pump-probe technique show the propagation of the phonon wave packet generated near the surface of the sample [3,4]. Under the present experimental condition, the penetration depth of the 360-nm pump pulse estimated from the absorption coefficient of $Al_{0.5}Ga_{0.5}As$ (~6.9×10^5 cm^{-1}) [6] is several tens nm and thinner than the total thickness of the constituent SL. The phonon wave packet is generated near the surface region with the skin depth of several tens nm, and propagates through the SL layer. The coherent phonon signals are detected within the propagation time of the phonon wave packet through the long-period SL, because the probe pulse with the wavelength of 720 nm picks up the coherent signals throughout the SL layer. The sudden disappearance of the time-domain signal in the long-

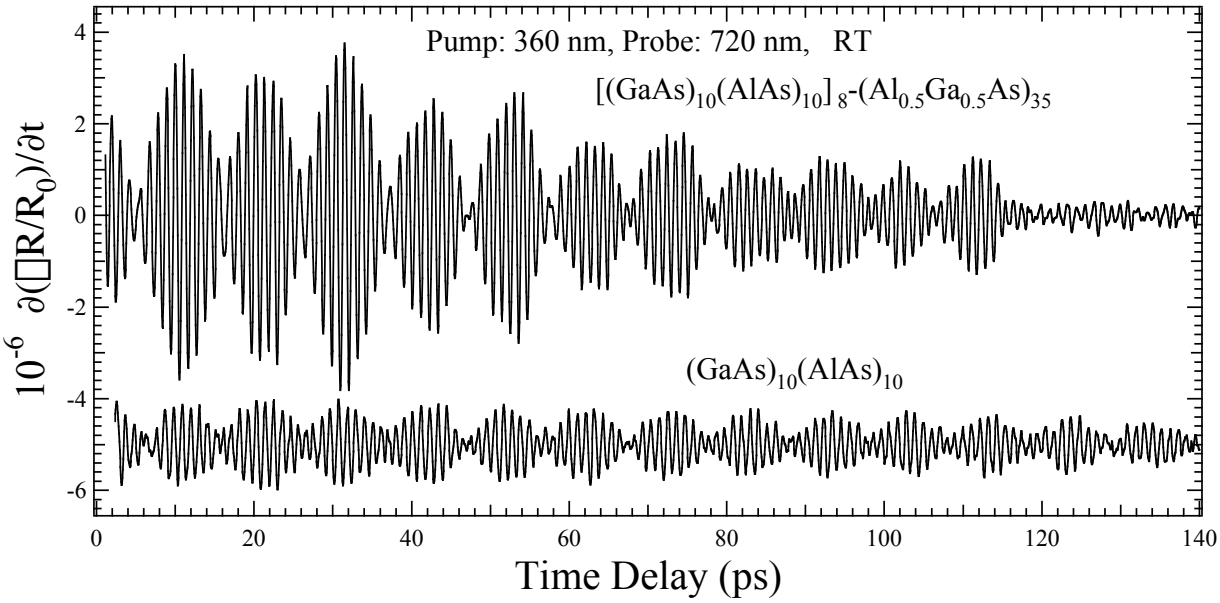

Fig. 2. Oscillatory parts of the time-derivative signals of the reflectivity change observed in the long-period SL (top) and the $(GaAs)_{10}(AlAs)_{10}$ SL (bottom).

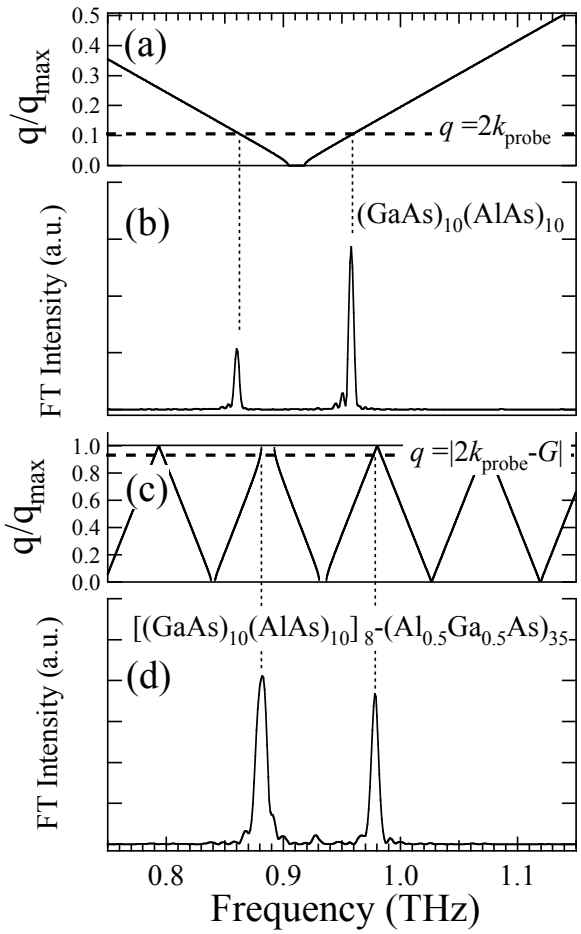

Fig. 3. FT spectra of the time-domain signals in (b) the $(GaAs)_{10}(AlAs)_{10}$ SL and (d) the long-period SL, and dispersion curves of the FLA phonon for (a) the $(GaAs)_{10}(AlAs)_{10}$ SL and (c) the long-period SL, calculated on the basis of an elastic continuum model.

period SL implies the escape of the phonon wave packet from the SL layer. The escape time in the long-period SL is calculated to be about 117 ps by using the sound velocity of 5.2×10^5 cm/s and the total thickness of 607 nm. This calculated value is in good agreement with the experimental result. In this calculation, the SL is regarded as an $Al_{0.5}Ga_{0.5}As$ alloy and the sound velocity is estimated by linear interpolation from those of GaAs and AlAs. On the other hand, the estimated escape time in the $(GaAs)_{10}(AlAs)_{10}$ SL is about 212 ps, which leads to the fact that the 2C pump-probe signal hardly decays in the time region less than 140 ps as shown in Fig. 1.

In order to analyze the coherent oscillation modes, we performed the FT of the time-domain signals as shown in Figs. 3(b) and 3(d). The FT spectrum of the time-domain signal in the $(GaAs)_{10}(AlAs)_{10}$ SL shows two peaks at 0.86 and 0.96 THz. In the long-period SL, two peaks are observed at 0.88 and 0.98 THz. Moreover, the spectral widths of the 0.88- and 0.98-THz modes observed in the long-period SL are about 5 and 3 GHz, respectively, while those of 0.86- and 0.96-THz modes in the $(GaAs)_{10}(AlAs)_{10}$ SL are almost the same value of 2 GHz. The spectral widths of the two peaks observed in the long-period SL is slightly larger than those in the $(GaAs)_{10}(AlAs)_{10}$ SL. The difference in the spectral width between the two SL's results from the differences of the dephasing time and the escape time of the phonon wave packet as mentioned above.

The peak frequencies are compared with the dispersion relation of the FLA phonon in order to assign the peaks observed in the FT spectra. Figures 3(a) and 3(c) show the dispersion relations of FLA phonon modes in the two SL's calculated using a transfer matrix method based on an elastic continuum model [7-9]. In Fig. 3(a), the horizontal broken lines show the wave vectors given by $q/q_{max} = 2k_{probe}/q_{max} = 4nD/\lambda$, where λ is the wavelength of the probe pulse. In the FT spectra of the $(GaAs)_{10}(AlAs)_{10}$ SL, the two peaks observed are clearly assigned to the FLA phonons with $q=2k_{probe}$. On the other hand, in the FT spectra of the long-period SL, the wave vector of the FLA phonons is $q/q_{max} \sim 0.93$ from comparison of the frequencies of the two peaks with the phonon dispersion, and this value does not coincide with the calculated value of $2k_{probe}/q_{max} \sim 1.07$. Taking the umklapp process into consideration, the wave vector of the propagating FLA phonon is presented by

$$q = |2k_{probe} - mG|, \qquad (1)$$

where $G=2\pi/D$ and m is an integer [8]. As shown in the horizontal broken line of Fig. 3(c), which indicates the value of the wave vector obtained by taking account of the umklapp process, the calculated wave vector, $q/q_{max}=0.93$, is in good agreement with the experimental one. This agreement demonstrates that the propagating FLA phonons in the long-period SL are observed through the umklapp process under the condition that the wave vector of the probe pulse in the sample exceeds the mini-Brillouin zone.

As shown in Fig. 3 (d), we note that the small peak is observed at 0.93 THz in the FT spectrum of the long period SL. This mode is assigned to the $q=0$ FLA phonon mode, i.e., the standing wave mode, by comparing the peak frequency with the dispersion relation of the FLA phonon shown in Fig. 3(c). One possible explanation for the appearance of the standing wave mode is considered as follows. The phonon wave packet propagating in the direction from the surface to the substrate will be slightly reflected at the interfaces between GaAs, AlAs and $Al_{0.5}Ga_{0.5}As$ layers by the small difference in the acoustic impedances, and the reflected wave will propagate in the opposite direction. When the wave vector of the FLA phonon is close to the condition to satisfy the Bragg

condition $q=2\pi/D$, the phonon wave packet propagating in a given direction will interfere with one propagating in the opposite direction, leading to a standing wave. The standing wave oscillation in the SL spatiotemporally modulates the dielectric constant, which induces the oscillatory signals in the time-resolved reflectivity changes through photoelastic effects [3,10].

4. Conclusion

Coherent FLA phonons in the GaAs/AlAs long-period SL which consists of alternate stacking of a $(GaAs)_{10}(AlAs)_{10}$ SL with 8 periods and a $(Al_{0.5}Ga_{0.5}As)_{35}$ layer have been investigated by using a reflection-type two-color pump-probe technique with the 360-nm pump pulse and 720-nm probe pulse. The oscillation components of the time-domain signals indicate the propagation of the phonon wave packet through the long-period SL. The FT spectrum of the time-domain signals demonstrates that the propagating FLA phonons in the long-period SL are detected through the umklapp process when the wave vector of the probe pulse exceeds the mini-Brillouin zone. The wave vector of the FLA phonons observed through the umklapp process is presented by $q=|2k_{probe}-mG|$.

Acknowledgement

This work was partially supported by a Grant-in-Aid for the Scientific Research from the Ministry of Education, Culture, Sports, Science, and Technology of Japan.

References

[1] T. Dekorsy, G. C, Cho, and H, Kurz, in '*Light Scattering in Solids VIII*', (*ed*.) M. Cardona and G. Güntherodt, (Springer, Berlin, 2000) Chap. 4.

[2] A. Bartels, T. Dekorsy, H. Kurz, and K. Köhler, Appl. Phys. Lett. **72** (1999) 2844. and Phys. Rev. Lett. **82** (1999) 1044.

[3] K. Mizoguchi, M. Hase, S. Nakashima, and M. Nakayama, Phys. Rev. **B60** (1999) 8262.

[4] K. Mizoguchi, H. Takeuchi, T. Hino, and M. Nakayama, J. Phys.: Condens. Matter **14** (2002) L103.

[5] R. Merlin, Solid State Commun. **102** (1997) 207.

[6] D. E. Aspnes, S. M. Kelso, R. A. Logan, R. Bhat, J. Appl. Phys., **60** (1986) 754.

[7] S. M. Rytov, Akust. Zh. **2** (1956) 71 [Sov. Phys. Acoust. **2** (1956) 68.]

[8] S. Nakashima, *et al*., Phys. Rev. **B41** (1990) 5221.

[9] B. Jusserand and M. Cardona, in '*Light Scattering in Solids V*', (*ed*.) M. Cardona and G. Güntherodt, (Springer, Berlin, 1989) Chap. 3.

[10] O. Matsuda, and O. B. Wright, J. Opt. Soc. Am. **B19** (2002) 3028.